April 2000

Chem. Pharm. Bull. **48**(4) 467—476 (2000)

467

Quantitative Analysis of the Kinetic Constant of the Reaction of N,N'-Propylenedinicotinamide with the Hydroxyl Radical Using Dimethyl Sulfoxide and Deduction of Its Structure in Chloroform

Toshio Akimoto*

Chemistry Research Lab., Fuji Gotemba Research Labs., Chugai Pharmaceutical Co., Ltd., 135, Komakado, 1 Chome, Gotenba-shi, Shizuoka 412–8513, Japan. Received August 11, 1999; accepted December 28, 1999

N,N'-Propylenedinicotinamide (Nicaraven) is presently being developed for the treatment of cerebral stroke including subarachnoid hemorrhage. This drug is promising because some data suggest it to have an ability to scavenge the hydroxyl radical under physiological conditions *in vivo*, while it also has a high permeability through the blood brain barrier.

Using the kinetic constant of the reaction between the hydroxyl radical and dimethyl sulfoxide, the formula derived by Babbs and Griffin (*Free Rad. Biol. Med.*, 6 1989) was applied to obtain the kinetic constant of Nicaraven with the hydroxyl radical using a dimethyl sulfoxide–xanthine oxidase–hypoxanthine–Fe system, and this yielded the kinetic constant $3.4 \times 10^9 \, M^{-1} s^{-1}$ ($1 \, M = 1 \, mol \, dm^{-3}$) for Nicaraven. Structurally related compounds were also investigated. The amide group of Nicaraven was thus found to play an important part in the reaction with the hydroxyl radical.

Methanesulfinic acid, which was obtained from the reaction between dimethyl sulfoxide and the hydroxyl radical, was found to be stable under this adopted experimental condition and therefore was used to quantify the kinetic constant of Nicaraven.

The structure of Nicaraven has also been investigated in CDCl₃ using IR spectra, computer calculations and ¹H-NMR analysis, and Nicaraven was thus shown to have an intramolecular hydrogen bond which forms a 7-membered ring that resembles a part of the 1H-1,4-benzodiazepines. This structure may play an important role in the penetration through the blood brain barrier.

Key words hydroxyl radical; dimethyl sulfoxide; blood brain barrier; xanthine oxidase; methanesulfinic acid; benzodiazepine

Oxygen radicals are produced in the brain during cellular respiration and their production accelerates dramatically during brain insult.[1] The most reactive radical, namely, the hydroxyl radical ($\cdot$OH) is able to oxidize proteins,[2] lipids[3] and nucleic acids.[2] It is therefore believed to be a very important property for potential drug therapy of brain insult to scavenge $\cdot$OH.

N,N'-propylenedinicotinamide (Nicaraven, Fig. 1) is presently being developed for the treatment of cerebral stroke including subarachnoid hemorrhage.[4,5] Nicaraven has been given to patients by intravenous drip, with four grams of the drug administered over an 8-h period, once per day for a period of 10 d in clinical trials. This drug is promising because data suggest it has an ability to scavenge $\cdot$OH under physiological conditions *in vivo*.[6,7] For example, Gidö and Wieloch demonstrated that the production of 3,4-dihydroxybenzoic acid (3,4-DHBA) from 4-hydroxybenzoic acid given to rats remarkably decreased soon after ischemia when the Nicaraven concentration was increased to 1 mg/ml/min after intravenous infusion.[6] Nicaraven also has high permeability through the blood brain barrier (BBB).[8]

Babbs and Griffin first reported a Scatchard plot analysis to determine the total $\cdot$OH production.[9] We used their slightly modified method to obtain the kinetic constant and this method proved to be very convenient, since no large apparatus was required such as is the case with electron spin resonance or gamma radiolysis. They also reported methanesulfinic acid (MSA) to be produced from a reaction of dimethyl sulfoxide (DMSO) and $\cdot$OH, and stated that MSA can be measured after diazotization.

We herein describe a method in which, after measuring the quantity of diazotized MSA and using the kinetic constant of

the reaction of DMSO with $\cdot$OH that had been obtained by gamma radiolysis, the kinetic constant of the reaction between a compound and $\cdot$OH could be obtained.

Although the MSA yielded from the reaction with DMSO cannot be regarded as a product derived with $\cdot$OH alone and other active oxygen species must also be taken into account according to the finding of Yamazaki and Piette,[10,11] the total yield of MSA was determined in this study and thereafter was used for the analysis.

Brain drugs need to penetrate the BBB and it is commonly believed that compounds with a high water solubility cannot do so.[12] Nicaraven, however, has a very high water solubility of 821 mg/ml, but nevertheless shows a good BBB penetration. Interestingly, this compound also dissolves in chloroform at 203 mg/ml. A structural analysis of Nicaraven in CDCl₃, which is a rather hydrophobic environment, was made using the IR absorption spectrum of N–H stretching vibration and a ¹H-NMR spectral analysis, while a semi-empirical quantum mechanical calculation was also performed.

The finding of a quantitative kinetic study with $\cdot$OH and the structure in CDCl₃ of Nicaraven are reported in this paper.
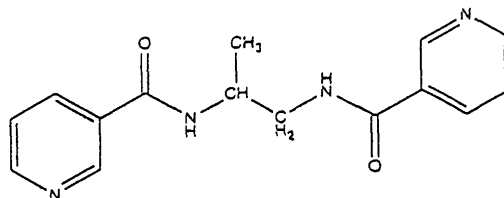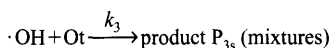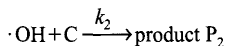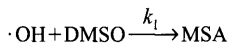

Fig. 1. Chemical Structure of Nicaraven

Theoretical Background for Obtaining a Kinetic Constant The mathematical formula for the Scatchard plot analysis proposed by Babbs and Griffin[9] has been modified as follows. In this formula, k_1, k_2 and k_3 are the kinetic constants when C is the test compound, e.g. Nicaraven, while Ot represents the other mixtures such as xanthine oxidase, etc.

$$\cdot OH + DMSO \xrightarrow{k_1} MSA$$

$$\cdot OH + C \xrightarrow{k_2} product\ P_2$$

$$\cdot OH + Ot \xrightarrow{k_3} product\ P_{3s}\ (mixtures)$$

The MSA produced by the attack of $\cdot OH$ is described by the equation below: The square brackets express the concentration.

$$[CH_3SOOH] = \alpha[\cdot OH] \cfrac{[DMSO]}{[DMSO] + \cfrac{k_2[C]}{k_1} + \cfrac{k_3[Ot]}{k_1}} \quad (1)$$

In this Eq. 1, α represents the coefficient of the MSA yield from DMSO and the diminishing factor of [MSA] by $\cdot OH$ attack.[13] When the DMSO concentration is high enough to capture all the produced $\cdot OH$, then $[\cdot OH]$ becomes $[CH_3SOOH]_{max}$ and α becomes nearly 1.0. Babbs and Griffin developed the mathematical formula noted below based on this hypothesis[9]:

When K is defined as

$$K = \frac{k_2[C]}{k_1} + \frac{k_3[Ot]}{k_1} \quad (2)$$

then

$$\frac{[CH_3SOOH]}{[DMSO]} = \frac{[CH_3SOOH]_{max}}{K} - \frac{[CH_3SOOH]}{K} \quad (3)$$

From the above Eq. 3, $1/K$ defined as Eq. 2 can be obtained from the slope of the straight line of $[CH_3SOOH]/[DMSO]$ and $[CH_3SOOH]$ which are plotted as the y-axis and x-axis, respectively. Using k_1, which represents the kinetic constant of the reaction between DMSO and $\cdot OH$ as $7 \times 10^9\,M^{-1}s^{-1}$,[14] and $k_3[Ot]/k_1 = 0$, if negligible, then, Eq. 2 can be reduced to $K = k_2[C]/k_1$.

To obtain the condition of $\alpha = 1$ and $[CH_3SOOH]_{max} = [\cdot OH]$ and if the effect of $k_3[Ot]/k_1$ can be regarded as negligible, then experiments in which [DMSO] and [MSA] have been changed in the absence of a test compound such as Nicaraven would have to be carried out (see Results). To successfully obtain a straight line in Scatchard plots, the appropriate range of the combination of [DMSO] and [C] must be determined. If [DMSO] is too high, then α in Eq. 1 would be greater than 1.0. This is because when the [DMSO] concentration is too high, the radical chain reaction between DMSO and the radical yielded from DMSO would cause an increased generation of MSA. If [DMSO] is too low, then α would become less than 1.0. This is because when [DMSO] is too low, the MSA generated from it is damaged by an $\cdot OH$ attack, and the effect of [Ot] also cannot be ruled out.

Experimental

Compounds Examined The compounds measured were Nicaraven, mannitol, N-methylnicotinamide (NM-NA), pyridine and N-methylac-etamide (NMAA). The reason these compounds were utilized first was to get information about which moiety of the Nicaraven molecule plays a key role in the reaction with $\cdot OH$. A second reason was to determine the precision of this analytical method by comparing the results with those already published elsewhere.

Materials and Experimental Procedures Materials: The diazo compound reacted with MSA was Fast Blue BB salt (azoic diazo component 20) which was purchased from Tokyo Kasei Co., Ltd. DMSO of ultra-pure grade was obtained from Wako Pure Chemicals Co., Ltd. The MSA sodium salt was from Lancaster Co., Ltd. Butter milk xanthine oxidase (E.C.1.2.3.2) 25 U/ml 60% ammonium sulfate suspension was also from Wako. All other chemicals used in this experiment were of reagent grade.

The Stock Solutions: Hypoxanthine was dissolved in 1.0 M (1 M = 1 mol dm^{-3}) NaOH to 40 mM and diluted to 133 μM in phosphate buffered saline (PBS, 100 mM NaCl, 50 mM phosphate buffer, pH7.4). Fe–EDTA was dissolved to 1.5 mM in PBS. DMSO was diluted in PBS to various concentrations ranging from 30 mM to 450 mM (7 points). Xanthine oxidase was diluted 30 times in PBS. The concentration of the compounds examined was 150 mM, respectively.

Experimental Procedures: The following experimental procedures for the kinetic analysis were similar to those carried out by Babbs and Griffin.[9]

The reaction was started by adding 0.2 ml xanthine oxidase (final concentration 56 mU/ml) into the mixture of 0.1 ml DMSO (1.0 mM to 15 mM in final), 0.1 ml of one of the compound solutions, 0.2 ml Fe–EDTA and 2.4 ml hypoxanthine solution. The blank for the optical density measurement had the same composition as the sample solution except 0.1 ml PBS was added instead of 0.1 ml DMSO solution. The final concentration of hypoxanthine was 106 μM, and the concentration of a test compound was 5.0 mM. The reaction was carried out under 20 min standing conditions after slight vortexing. Regarding Nicaraven, the final concentration of 10 mM was also investigated.

Thereafter, the solution was treated in a similar way to that by Babbs and Griffin.[9]

Damage of MSA by $\cdot OH$ To examine the behavior of the MSA exposed to $\cdot OH$ under these experimental conditions, authentic MSA was added instead of DMSO from the beginning and the optical density was measured. The authentic MSA was also measured after the chemical treatment described above in the absence of xanthine oxidase for comparison purposes.

DMSO Concentration to Protect Yielded MSA From the above experiment, the MSA generated under experimental conditions was destroyed by the $\cdot OH$ attack if the DMSO concentration was too low to react with all of the $\cdot OH$. To further elucidate this problem, certain concentrations of MSA were added to the experiment beforehand and the decay rate of MSA was observed by changing the DMSO concentrations. The concentrations of MSA added beforehand were 0, 11, 22, 38.5 and 55 μM in the final concentration. The DMSO concentrations were 0.47, 0.93, 4.67 and 9.33 mM in the final concentration.

Protection of Yielded MSA by the Combination of DMSO and a Compound Furthermore, the same problem (MSA damage by $\cdot OH$) could occur when a test compound such as Nicaraven is added. To obtain information on this effect, a DMSO concentration of 0.47 mM and a Nicaraven concentration of 3.3 mM, a DMSO concentration of 0.47 and 0.94 mM and mannitol 3.3 mM were tested using MSA at the same concentrations as those noted above, which was added before the xanthine oxidase was added.

Scatchard Plot Analysis After a careful examination of the above results (see Results), a Scatchard plot analysis was carried out using the 5.0 mM test compound and DMSO solution with a concentration of 1.0, 1.67, 2.5, 3.3, 6.67, 10.0 and 15.0 mM.

Reactive Site of Nicaraven with $\cdot OH$ The Fenton reaction using Fe^{III} was applied[15] to determine which moiety of Nicaraven reacts with $\cdot OH$. The PBS used had the same composition as that used throughout this work. The final concentration of Nicaraven was 10 mM, while that of Fe–EDTA is 2.0 mM, and the concentrations of H$_2$O$_2$ were 0, 8.8 and 13.2 mM. The 100 ml mixed solution was left standing for 4 to 5 d. After freeze-drying this mixture, the IR and ^{1}H-NMR spectra were measured. Preparation of DMSO-d_6 solution of freeze-dried sample to measure the ^{1}H-NMR spectrum required filtration. The NMR apparatus used was a JNM-EX270 of JEOL.

From the samples obtained in the same manner as described in the preparation above (freeze-dried sample), extraction was carried out using 120 ml of dichloromethane, after which the insoluble part was dissolved in water and adjusted to pH 10.0 by sodium hydrogencarbonate, and then freeze-dried. Thereafter the extraction was done using 120 ml of dichloromethane. After obtaining an insoluble part by filtration, the extraction was carried out

using 100 ml ethanol. These three solutions for the extraction were evaporated to dryness at 40 °C. TLC ($CHCl_3$: methanol=5 : 1 and $CHCl_3$: methanol=5 : 1 plus one drop of acetic acid), and then the measurement of ^{1}H-NMR in DMSO-d_6 and IR in the KBr disk were carried out.

Structural Study of Nicaraven A structural study of IR absorption measurement was carried out using a Horiba 730 FT-IR spectrometer. The concentrations of Nicaraven were 30, 10, 3 and 0.5 mM in $CDCl_3$ and that of NM-NA was 10 mM in $CDCl_3$. The solution cell had a KBr window with spacing of 0.5 mm.

Molecular dynamics calculation was carried out using the Discover version 2.9.7 software package of Molecular Simulation, Inc. U.S.A., and every 2.5 psec, the structure was selected for simulated annealing from 900K to 300K for one psec. Successive 4 psec dynamics calculations were made at 300K, after which a total of 10 structures were geometry-optimized using molecular mechanics. One of the structures, which had two closed pyridine rings in a stack, even though a complete stacking of the two pyridine rings of this molecule is not possible, was geometry-optimized using the semi-empirical quantum mechanical program package MOPAC, version 6.0.[16] PM3 Hamiltonian was applied in this study. The hardware used was IRIS Indigo2 and Power Challenge from Silicon Graphics.

To confirm the structure obtained by both IR absorption observations and a PM3 calculation study, a ^{1}H-NMR study was carried out on Nicaraven concentrations of 2 and 20 mM in $CDCl_3$. The signals of the two methylene protons of Nicaraven appeared at different resonant positions. Based on the calculated structures by PM3, the Karplus equations were applied to support the correctness of the calculated structures. The Karplus equations used were for the peptide analysis and are expressed as follows.

$$^3J_{HNC_\alpha H} = 9.4 \cos^2\theta - 1.1 \cos\theta + 0.4^{17)}$$

$$^3J_{HC_\alpha C_\beta H} = 9.4 \cos^2\theta - 1.4 \cos\theta + 1.6^{18)}$$

To assign a coupling constant to each proton pair, the homo-decoupling measurements to two amide protons and to methyl protons were applied using a Varian Mercury 300. When measuring the 2 mM solution, a Bruker DRX750 was used.

Results

Determining the Total [·OH] Production By putting MSA instead of DMSO directly into the experimental reaction, the linearity of absorbance to the [MSA] exposed to ·OH was confirmed, and the linearity was good. However, the slope of absorbance/[MSA] under experimental conditions was only 1/3 that of the MSA measured in the absence of xanthine oxidase (data not shown).[13]

Figure 2 shows the absorbance at 425 nm when the known

concentrations of MSA were added before the xanthine oxidase was added to the solution. In this case, no test compound to investigate the kinetics was added. The slope of the upper two straight lines was saturated because that with DMSO 4.67 mM was steeper than that with 9.33 mM and the two y-intersections of the straight lines were equal within the range of experimental error. Furthermore, the slopes of these two lines closely coincided with the slope of the line which was drawn when the given concentration of MSA was mixed with PBS (MSA alone in Fig. 2). By averaging 2 straight lines of the y-intersections, the equation can be expressed as

$$y = 0.122 + 2.36 \times 10^{-3} x$$

Here, y is the absorbance and x is MSA added with the unit of μM. This DMSO concentration region can be interpreted as follows: The added MSA was well protected from decay, because all the hydroxyl radicals were consumed by the large concentration of DMSO. The y-axis intersection is expected to be $[\cdot OH] = [CH_3SOOH]_{max}$ and $\alpha = 1$ in the Eq. 1. The slope of this linear equation must be proportional to the added MSA concentrations. Using the above equation, the total $[\cdot OH] = [CH_3SOOH]_{max}$ was determined as 53 μM when 106 μM hypoxanthine was added. Fifty-three μM MSA corresponded to the absorbance 0.122, and thus $x = 437y$ could be obtained. Here, x is MSA μM and y is the absorbance obtained.

The slopes at DMSO 0.93 mM and 0.47 mM were less than those of DMSO 4.67 and 9.3 mM. This means the MSA yielded from DMSO concentration 0.93 or 0.47 mM is partly destroyed by ·OH. At these concentrations of DMSO, MSA is not stable and the effect of [Ot] cannot be disregarded.

Appropriate Combination of Concentrations of DMSO and Test Compound The upper three lines of Fig. 3 show the behavior of the straight line when Nicaraven or mannitol 3.3 mM is added to the reaction tube, with DMSO at concentrations of 0.47 mM or 0.94 mM and MSA at certain known concentrations. If [Nicaraven] or [mannitol] and [DMSO] are high enough to capture all the ·OH yielded in the reaction, then the slopes of these lines should be equal to that of MSA
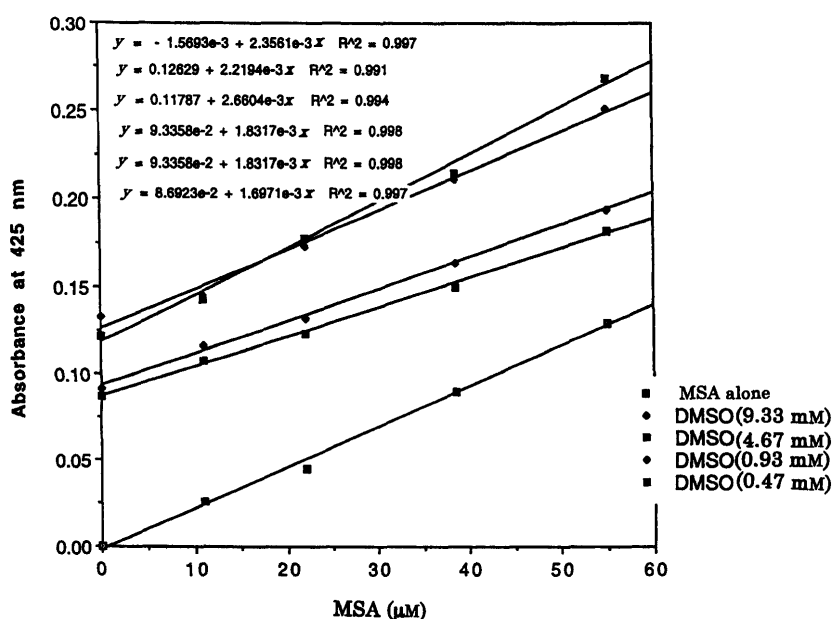

Fig. 2. The Effect of MSA Added beforehand to the Experimental Condition
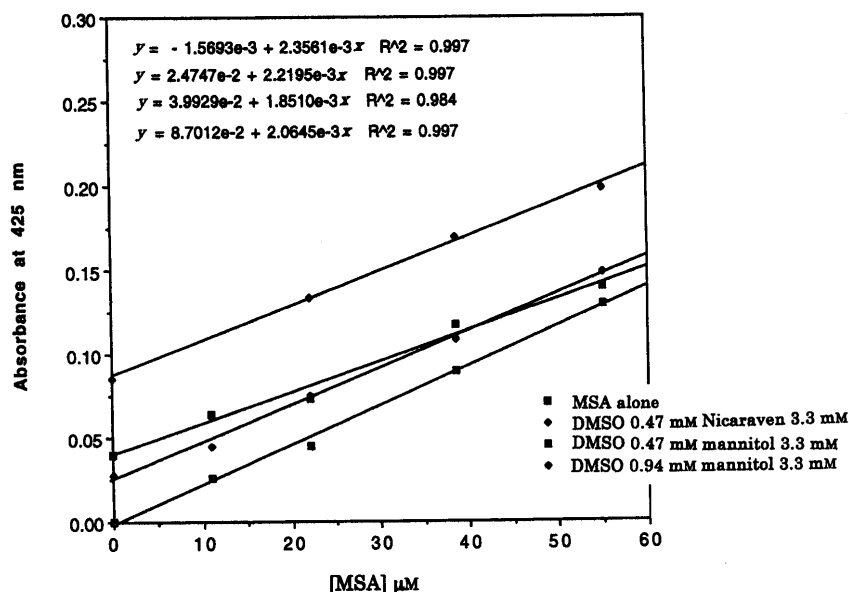
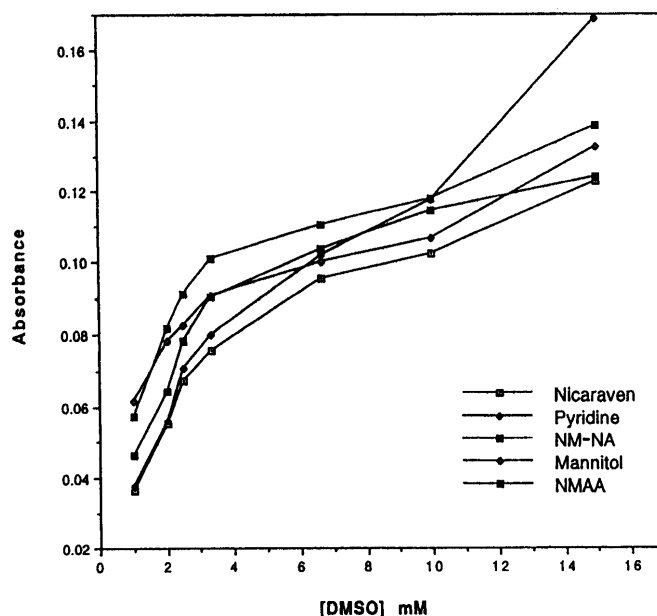Fig. 3. MSA Linearity at Different DMSO Concentrations When a Compound is Added

Fig. 4. The Absorbance Change When [DMSO] is Changed

alone in Fig. 3. From this point of view, the concentrations of 0.47 mM DMSO with 3.3 mM Nicaraven, and 0.94 mM DMSO with 3.3 mM mannitol would seem to be almost applicable to the Scatchard plots. However, the concentration of DMSO 0.47 mM with mannitol 3.3 mM is clearly unusable for the plot. From these results, the experimental conditions with a higher concentration of the test compound (5 mM) and higher concentrations of DMSO (more than 1.0 mM) have been employed to obtain the kinetic constant of each compound.

Scatchard Plot Analysis The absorbance vs. [DMSO] with each compound at a concentration of 5 mM is shown in Fig. 4.

The Scatchard plot of each compound was applied. As derived before, [MSA] μM$=437\times$absorbance; the value of $[CH_3SOOH]_{max}$, 53 μM was also used. This value was added to obtain the Scatchard plot for each compound, namely, [MSA]$=53$ μM and [MSA]/[DMSO]$=0.0$ was employed to

fit the straight line to each compound. If the measured [MSA] was greater than 53 μM, the point was omitted from the Scatchard plot. In this experiment, only DMSO 15 mM data had to be omitted. These data not only gave more than 53 μM of MSA, but also deviated from the straight line of the Scatchard plot (data not shown). This fact indicates that DMSO and the radical yielded from DMSO by ·OH attack thus yield extra MSA when more than 15 mM DMSO is used. The Scatchard plots of Nicaraven are shown in Fig. 5, and those of the other compounds in Fig. 6. By using each slope ($-1/K$) and $K=k_2[C]/k_1$, k_2 value of each compound was calculated. The results are shown in Table 1.

The kinetic constant of 10 mM of Nicaraven is also exhibited in Table 1.

When sterilized water was added which contained none of the detectable metallic ions used for making PBS and no Fe–EDTA, that is, when no metals were involved in this ex-
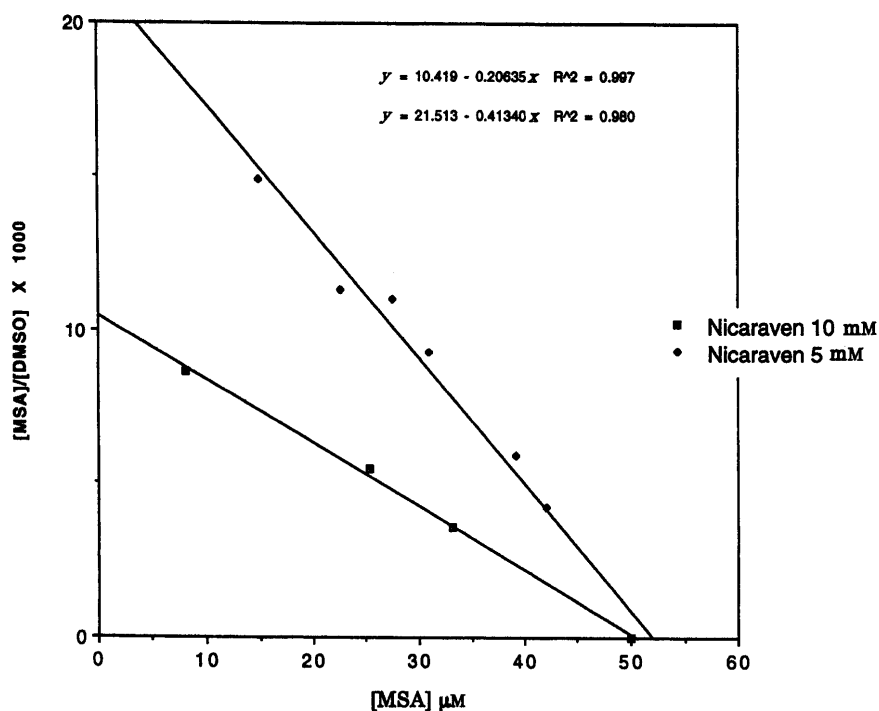
$y = 10.419 - 0.20635x$ R^2 = 0.997

$y = 21.513 - 0.41340x$ R^2 = 0.980

■ Nicaraven 10 mM
♦ Nicaraven 5 mM

[MSA]/[DMSO] X 1000

[MSA] μM

Fig. 5. Scatchard Plots of Nicaraven

$y = 23.118 - 0.38432x$ R^2 = 0.919

$y = 31.531 - 0.55163x$ R^2 = 0.943

$y = 52.662 - 1.0248x$ R^2 = 0.980

$y = 48.180 - 0.84769x$ R^2 = 0.949

■ Pyridine
♦ NM-NA
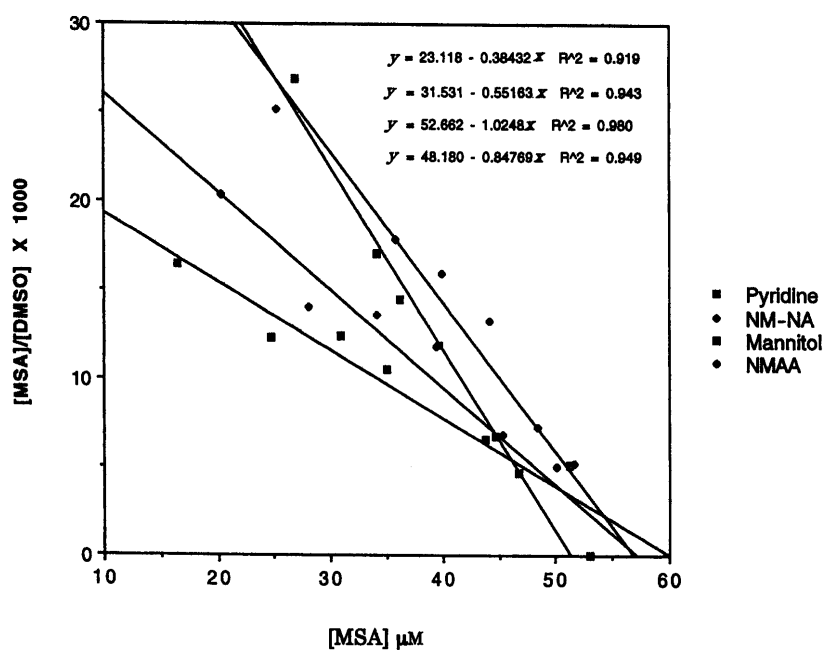■ Mannitol
♦ NMAA

[MSA]/[DMSO] X 1000

[MSA] μM

Fig. 6. Scatchard Plots of the Other 4 Compounds

Table 1. Kinetic Constants Obtained from Scatchard Plots

	$\times 10^9 \, M^{-1} s^{-1}$	Slope $\times 10^3 \, M$	Literature value for k_2 $\times 10^9 M^{-1} s^{-1}$
Nicaraven	3.4	−0.415	
Pyridine	3.6	−0.384	4.5[19]
Mannitol	1.4	−1.025	1.0—1.8[20]
NM-NA	2.5	−0.552	
NMAA	1.7	−0.848	1.6[21]
Nicaraven (10 mM)	3.4	−0.208	

The slope is the coefficient of the Scatchard plots $(-1/K)$. The drug concentration is always 5.0 mM, except for the Nicaraven on the last line in which the drug concentration is 10 mM.

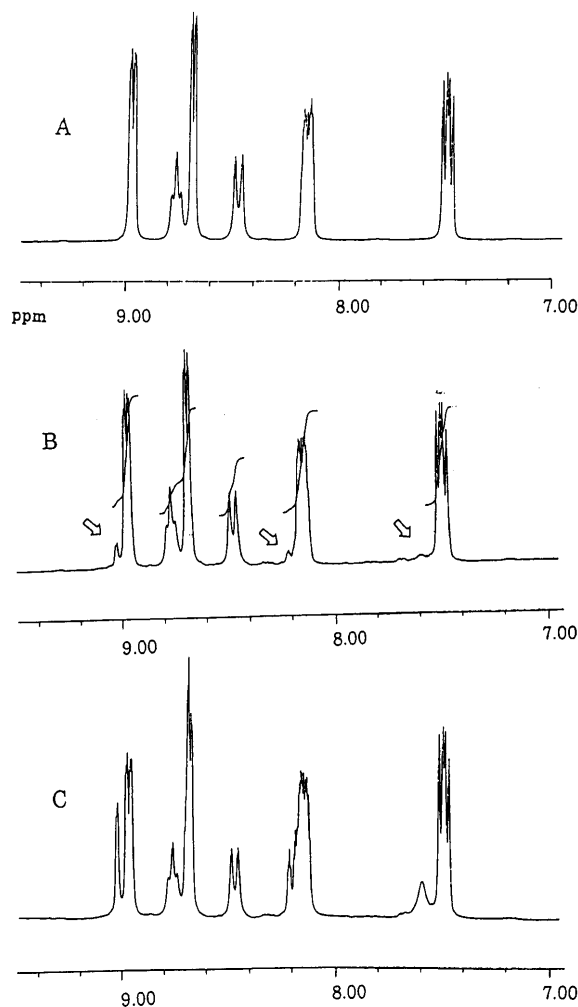periment, no meaningful amount of MSA was detected.

The Reactive Site of Nicaraven with ·OH Solvent extraction was carried out to learn which moiety of Nicaraven is attacked by ·OH (see Materials and Method). The extracted weight after drying by a vacuum pump is shown in Table 2.

Nicaraven has two possible sites where the hydroxyl radical attacks; pyridine moiety[22,23] and amide moiety.[24—26] Pyridine is known to be changed to pyridinol by an ·OH attack.[22,23] Generally speaking, the phenolic proton shows signals of a higher field than 9.5 ppm on the ^{1}H-NMR spectrum, while when the amide moiety is attacked by ·OH, nicotinic acid or nicotinamide is yielded; because amino acid[24,25] or

Table 2. Weight (mg) of Each Extract when 284 mg of Nicaraven Is Used

	H_2O_2 concentration (mM)		
	0.0	8.8	13.2
CH_2Cl_2 extract (1)	280.0	209.0	186.7
CH_2Cl_2 extract (2)	11.0	28.6	25.4
Ethanol extract	81.7	71.7	81.1

See Experimental for the extraction scheme.

Table 3. The Ratio of the Strength of Absorptions Due to Stretching Vibrations of Hydrogen Bonded N–H at 3340 cm^{-1}/Free N–H at 3450 cm^{-1}

Nicaraven conc. (mM)	Absorbance ratio A_{3340}/A_{3450}
30	1.47
10	1.04
3	0.78
0.5	0.73

Fig. 7. ^{1}H-NMR Spectra for the Identification of Nicotinamide

A: Nicaraven, B: dichlorometane extract 2. Nicotinamide signals are shown with arrows. C: small amount of nicotinamide is added to B.

amino acid amide[26] has been hypothesized to result from protein degradation by an ·OH attack.

The search for nicotinic acid and nicotinamide was carried out by ^{1}H-NMR measurements by adding small amounts of these compounds to each extract, and non-addition and post-addition samples were compared. Nicotinamide was found from two dichloromethane extracts as shown in Fig. 7. In a pre-search of these compounds, nicotinamide was identified on TLC (data not shown).

The nicotinamide molar content found in this ^{1}H-NMR measurement was roughly 1/7 that of Nicaraven from the integration of the spectrum of dichloromethane extracts 1 and 2, because the signal strength ratio of pyridine proton of nicotinamide to Nicaraven is about 1/15 when 13.2 mM of H_2O_2 to 10 mM of Nicaraven was used. In contrast, no nico-

tinic acid was found in either ^{1}H-NMR or TLC.

No phenolic proton could be found on the ^{1}H-NMR spectra of three extracts and the freeze dried sample before the extraction was applied.

The ethanol extract showed a rather broad ^{1}H-NMR spectra (data not shown) even after the re-extraction by 2-propanol to avoid extracting inorganic compounds (data not shown). In this case, the residual 2-propanol showed sharp spectra.

It can thus be concluded that the amide groups of Nicaraven play an important role in reacting with ·OH. Other reports mention that the polymerization and precipitation of proteins occur after an ·OH attack under oxygen free conditions.[27,28]

Structure Determination of Nicaraven in CDCl$_3$ The structure in CDCl$_3$ was obtained after measuring the N–H stretching vibration and calculating the semi-empirical quantum mechanics. Below the 3 mM concentration levels of Nicaraven, the ratio of the strengths of the stretching vibrations of the hydrogen bonded N–H (3340 cm^{-1}) to free N–H (3450 cm^{-1}) is almost constant, as shown in Table 3. This means that at concentrations below 3 mM, the Nicaraven molecule has no intermolecular hydrogen bond and the dominant structure of Nicaraven has an intramolecular hydrogen bond. The 3 mM IR spectrum is shown in the upper part of Fig. 8. The spectrum of 10 mM NM-NA in the lower part of Fig. 8 is seen to have almost no intermolecular hydrogen bond.

Three of the ten structures had an intramolecular hydrogen bond after simulated annealing and the successive geometric optimization using molecular mechanics (data not shown). Although there are four possible structures having an intramolecular hydrogen bond, only two structures are possible which have a methine proton and one of the methylene protons is in the *trans* position (from ^{1}H-NMR measurement, see below); therefore, we do not have to consider two structures whose methyl groups are axial to a 7-membered ring formed by an intramolecular hydrogen bond. These two possible structures are shown in Fig. 9. PM3 calculation showed the upper structure of Fig. 9 to be more stable by 2.0 kcal/mol. The most stable conformation by PM3 calculation is called model I and the less-stable structure is called model II in Fig. 9.

The two different NMR signals of two methylene protons were observed for a CDCl$_3$ solution of Nicaraven as shown in the upper part of Fig. 10, which supports the IR measurements in that the main molecular structure has an intramolecular hydrogen bond. The spectrum in a more polar solvent such as DMSO-d_6 however, does not show intra-molecular hydrogen bonding as in the lower part of Fig. 10. Based on the observed coupling constants obtained in CDCl$_3$, the dihedral angles were calculated for models I and II using the
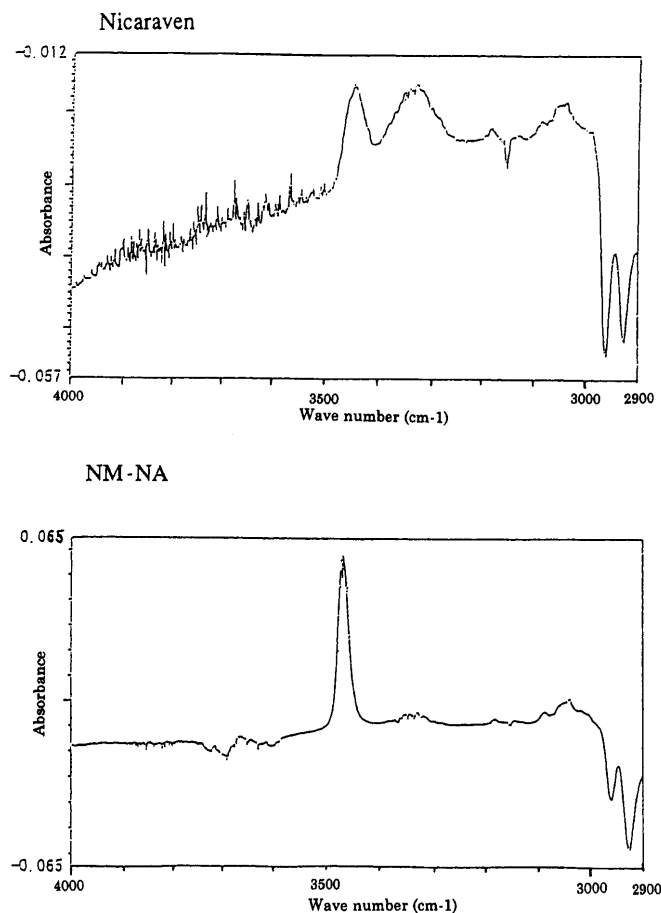
Fig. 8. IR-Spectrum of N–H Stretching Vibration of 3 mM Nicaraven in the Upper Part of the Figure and of 10 mM NM-NA in the Lower Part
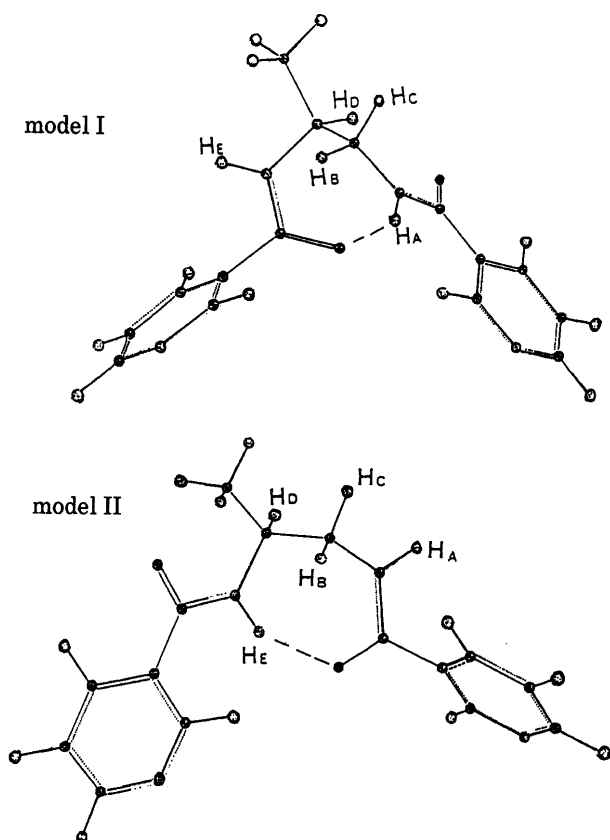

Fig. 10. ¹H-NMR Spectra

Upper: 20 mM Nicaraven in $CDCl_3$. Lower: 20 mM Nicaraven in DMSO-d_6.

Fig. 9. Two Optimized Structures of Nicaraven by PM3

Each proton is named as shown.

Karplus equations given before. These results are given in Table 4. It was found that the structure of model II can be disregarded due to the disagreement of the observed and calculated HNCH angles. Although the HANCHB angle does not agree with the observed value for model I, the other dihedral angles are closely similar to the observed values. The Karplus equations used in this calculation have been established from rigid molecules and for peptides. In this case, as only one hydrogen bond was seen to contribute to the cyclic structures, some disagreement between the observed and calculated dihedral angles may be permissible because the dynamic motion of the Nicaraven molecule could occur in $CDCl_3$. From the ¹H-NMR measurement, the model I structure could be hypothesized to be a main structure in chloroform, and this structure of Nicaraven was maintained even under concentrations as high as 20 mM.

The methylene signals at various concentrations of Nicaraven measured by JNM-EX270 are shown in Fig. 11. Signals at lower and upper fields are assigned to HB and HC, respectively. By decreasing the concentration of Nicaraven, the center of the HB proton shifts slightly down-field while that of the HC proton shifts slightly up-field and the spectra become complex at low concentrations. For this reason, we used DRX750 to obtain coupling constants at 2 mM. Although slight chemical shifts were observed when Nicaraven concentrations were changed, the main features of the spectra

Table 4. Coupling Constants Observed in this Experiment

	J_{OBS} (20 mM)	Angle (20 mM) from Karplus equation	J_{OBS} (2 mM)	Angle (2 mM) from Karplus equation	Angle of model I	Angle of model II
H_ANCH_B	6.6—6.9	±138—142	6.7	±142	−102.14	123.28
H_ANCH_C	4.6—4.7	±42—44	4.8	±44	142.30	8.41
		±128—130		±132		
H_BCCH_D	9.8—9.9	0	9.9	0	166.49	173.79
		±150—160		±150		
H_CCCH_D	3.6	±55	3.2	±60	−76.79	−69.85
H_DCNH_E	6.9	±142	5.0	±130	133.66	−114.67

The concentrations of Nicaraven are 20 and 2 mM. Based on the coupling constants, the dihedral angles were calculated using the equations noted in Experimental. The dihedral angles of model I and model II are shown in the Table. J_{OBS} 20 mM of H_DCNH_E was obtained from methine proton signals by the HOMO spin decoupling to methyl protons and H_E proton signals. J_{OBS} of 2 mM was obtained from H_E proton signals.
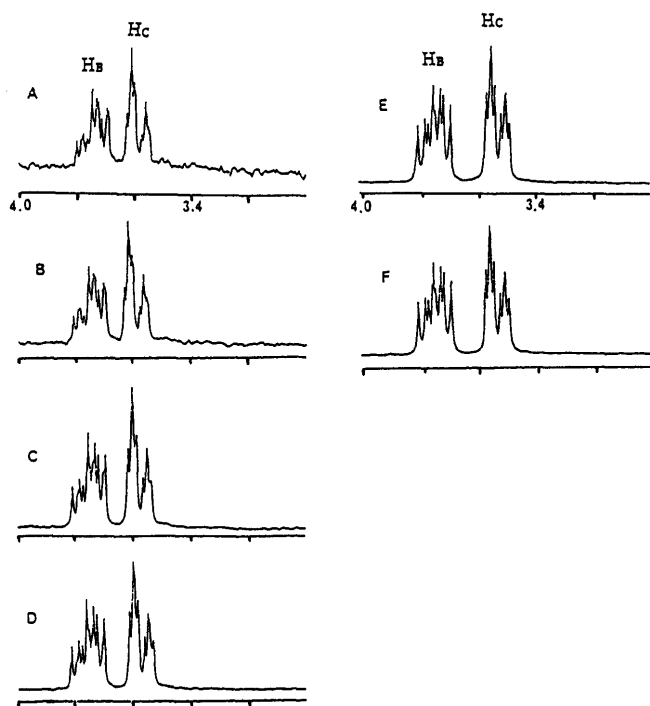

Fig. 11. The Methylene Signals of Nicaraven in $CDCl_3$ with the Change of Its Concentrations

A: 1 mM, B: 2 mM, C: 3 mM, D: 5 mM, E: 10 mM, F: 20 mM.

were very similar and no sudden conformational change was observed.

Discussion

Experimental Accuracy and Scavenging · OH by Nicaraven The k_2 values of this experiment are in good agreement with those of the literature cited as shown in Table 1. Although a relatively high concentration of the compound was needed in this experiment, we were able to relatively easily obtain the value of k_2 by the method described in this paper.

The kinetic constant of the reaction obtained in this experiment between Nicaraven and ·OH seems relatively small when Nicaraven is regarded as a direct scavenger of ·OH. However, we do not have enough environmental information on brain in disease, nor do we have sufficient local information about the Nicaraven molecule. We must take into account the complex formation ability of Nicaraven to an isolated iron atom, although the ability of the complex formation of Nicaraven with iron is substantially weaker than that

of EDTA with iron (data not shown). This fact might support the possibility that Nicaraven molecules tend to be located near iron atoms. In particular, a pyridine nitrogen atom can bind with an iron atom and the Nicaraven molecule can react rapidly with ·OH as soon as it is produced from an iron atom owing to the short distance between an iron ion and a Nicaraven molecule. Thus, the relatively high concentration of Nicaraven around an iron ion might be expected in the natural body. It may thus be concluded that the kinetic constant is a very important factor, but we also have to consider local distance and local concentration information whenever we deal with problems including reactions with ·OH.

Furthermore, Yamazaki and Piette found that the efficacy of ·OH generation varied with the nature of the iron chelators used.[11] Nicaraven–iron complex may decrease the total ·OH production.

It is noteworthy that the studies on oxygen free radicals and iron in biology and medicine have been reviewed by Halliwell and Gutteridge.[29]

Further investigations on the complex formation of Nicaraven with iron and on the efficacy of ·OH generation of the complex are therefore necessary.

Deoxyribose Method and This Method Halliwell et al. reported a simple "test-tube" assay to determine the rate constants using deoxyribose for reactions with hydroxyl radicals.[30] Their method does not require any complex pipette operations and may be more reliable than this method.

Their method can be briefly summarized as follows:

2-Deoxy-D-ribose (DR) is degraded on exposure to ·OH produced by Fenton systems. If the resulting complex mixture of products is heated under acidic conditions, malonaldehyde (MDA) is formed and can be detected by its ability to react with thiobarbituric acid (TBA) to form a pink chromogen, namely:

·OH+DR→fragments→MDA

2TBA+MDA→chromogen

Any other molecule S added to the reaction mixture that is capable of reacting with ·OH should compete with DR for ·OH to an extent dependent on its rate constant for reaction with ·OH and its concentration relative to DR .

the rate of reaction of DR with the hydroxyl radical $= k_{DR}[·OH][DR]$

the rate of reaction of S with the hydroxyl radical $= k_S[·OH][S]$

As a result, Halliwell et al. finally derived

$$\frac{1}{A} = \frac{1}{A_0}\left(1 + \frac{k_S[S]}{k_{DR}[DR]}\right)$$

where A is the absorbance in the presence of a scavenger S at concentration [S] and A_0 is the absorbance in the absence of a scavenger. Hence, a plot of $1/A$ against [S] should give a straight line of slope $k_S/k_{DR}[DR]A_0$ with an intercept on the y-axis of $1/A_0$, and the rate constant for the reaction of S with the hydroxyl radical can be obtained from the slope of the line. They used k_{DR} as $3.1 \times 10^9 \, M^{-1}s^{-1}$ obtained by gamma radiolysis and [DR] of more than 2.8 mM.

Halliwell *et al.* stressed the linearity of the straight line plot of the compound concentration, and the inverse of absorbance as x and y-axes, respectively, guarantees the usefulness of their method. Indeed, many compounds have been tested in this way with consistently good results.[30] However, their report does not touch upon the damage of the products yielded from DR by ·OH attack. Actually, it was shown by Parij *et al.*[31] that nonlinear competition plots were observed in several nonsteroidal anti-inflammatory drugs when the amount of [DR] used was 2.8 mM, and linear plots were observed when the amount of [DR] was 15 mM.

The method established by Halliwell *et al.* can analyze the change in the kinetic constant due to a change in the concentration of a compound, namely, the concentration dependency of a kinetic constant, can be analyzed. However, we have to consider that this kind of dependency could occur only when molecular interaction or molecular conformation changes happen at low concentrations of a compound in an aqueous solution. Such changes are considered to be rare. For this reason, an analysis at a fixed concentration of [S] while changing [DR] or [DMSO] could be worth future study.

Reactive Site of Nicaraven with the Hydroxyl Radical From the Fenton reaction samples, it was found that the amide group plays an important role in reactions with ·OH. Furthermore, Hu *et al.* determined the k_2 of nicotinic acid to be $0.68 \times 10^9 \, M^{-1}s^{-1}$.[32] In addition, the cumyloxyl radical ($C_6H_5C(CH_3)_2O\cdot$) was found by laser flash photolysis to attack the amide moiety of N-isopropylnicotinamide.[33] These facts suggest the pyridine ring of nicotinic acid derivative is not easily attacked by ·OH.

MSA Stability in This System Scaduto reported that the determination of MSA formation from DMSO underestimates the product of ·OH, because MSA is further oxidized by ·OH to methanesulfonate.[13] However, more than 5 mM of DMSO protects 100 μM MSA completely in this experiment, when the total [·OH] is around 50 μM. This means that DMSO could be a good indicator of ·OH in *in vivo* experiments, although there are some difficulties in obtaining total [·OH] as mentioned before. Actually there are several valuable *in vivo* reports.[34—36]

Nicaraven Penetration through BBB The permeability of Nicaraven into the brain is fairly good.[7] The structures of brain drugs have been summarized,[37] and both the bulkiness and the ring structures of these drugs appear to be quite important factors. Nitrogen atoms are also included more often in the structures than oxygen atoms. A chain structure is quite rare for a brain drug. Seelig *et al.* measured the surface area of the brain drugs and found that it is smaller than that of BBB non-penetrable drugs when they are of similar molecular weight.[38]
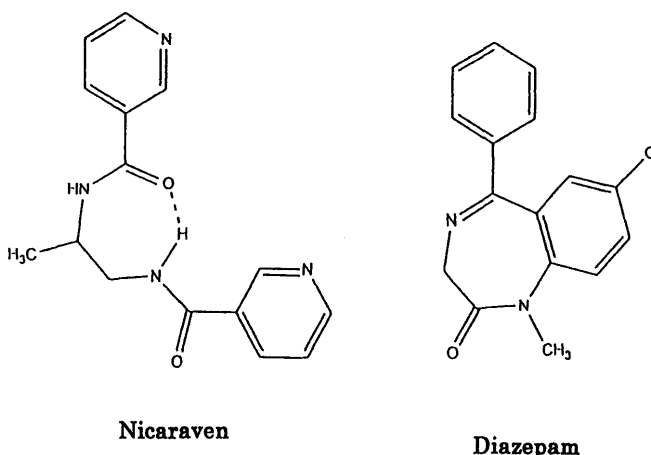

Nicaraven **Diazepam**

Fig. 12   Schematic View of Nicaraven and One of the Benzodiazepins, Diazepam

The PM3 calculation as well as the measurement of the IR and ^{1}H-NMR spectra are very interesting because the structure can be seen to partly resemble benzodiazepines, as shown in Fig. 12. The methyl in the propylene group of Nicaraven stabilizes the 7-membered ring by the 1—4 atom repulsive interaction. This could mean that Nicaraven assumes a similar, benzodiazepine-like structure when penetrating the BBB.

The benzodiazepine transporter in the brain is not known at present. There might be no specific transporter for benzodiazepines, although there are reports on the benzodiazepine inhibition of nucleoside transport in human erythrocytes[39] and on the benzodiazepine inhibition of triiodothyronine accumulation in human neuroblasts.[40] However, the concentrations of benzodiazepines in the brain are more than twice that in the total blood.[41] This fact suggests the importance of having a benzodiazepine-like structure which is able to penetrate the BBB.

References
1) Wilson J. X., *Can. J. Physiol. Pharmcol.*, **75**, 1149—1163 (1997).
2) Floyd R. A., Carney J. M., *Ann. Neurol.*, **32**, Suppl: S22—7 (1992).
3) Hall E. D., *Neurosurg. Clin. N. Am.*, **8**, 195—206 (1997).
4) Asano T., Takakura K., Sano K., Kikuchi H., Nagai H., Saito I., Tamura A., Ochiai, C., Sasaki T., *J. Neurosurg.*, **84** 792—803 (1996).
5) Germano A., Imperatore C., D'Avella D., Costa G., Tomasello F., *J. Neurosurg.*, **88**, 1075—1081 (1998).
6) Gidö G., Wieloch T., in preparation.
7) Bernnett J. P., Smith T. S., Naito S., in preparation.
8) Kamiyama H., Aso Y., in preparation.
9) Babbs C. F., Griffin D. W., *Free Rad. Biol. Med.*, **6**, 493—503 (1989).
10) Yamazaki I., Piette L. H., *J. Am. Chem. Soc.*, **113**, 7588—7593 (1991).
11) Yamazaki I., Piette L. H., *J. Biol. Chem.*, **265**, 13589—13594 (1990).
12) Koller W.C., *Neurology*, **36**, 1147 (1986).
13) Scaduto R. C., *Free Rad. Biol. Med.*, **18**, 271—277 (1995).
14) Cederbaum A. I., Dicker E., Rubin E., Cohen G., *Biochem. Biophys. Res. Commun.*, **78**, 1254—1262 (1977).
15) Gutteridge J. M. C., Wilkins S., *Biochim. Biophys. Acta*, **759**, 38—41 (1983).

16) Stewart J. J. P., *J. Comput. Aided Mol. Des.*, **4**, 1—105 (1990).
17) Bystrov V. B., *Progress in NMR Spectroscopy*, **10**, 44—81 (1976).
18) Kopple K. D., Wiley G. R., Tauke R., *Biopolymers*, **12**, 627—636 (1973).
19) Cohem H., Meyerstein D., *J. Chem. Soc. Dalton*, **1976**, 1976—1979.
20) Goldstein S., Czapski G., *Int. J. Rad. Biol.*, **46**, 725—729 (1984).
21) Hayon E., Ibata T., Lichtin N. N., Simic N., *J. Am. Chem. Soc.*, **92**, 3898—3903 (1970).
22) Steeken S., *J. Phys. Chem.*, **82**, 372—374 (1978).
23) Selvarajan N., Raghavan N. V., *J. Phys. Chem.*, **84**, 2548—2551 (1980).
24) Rana T. M., Meares C. F., *J. Am. Chem. Soc.*, **112**, 2457—2458 (1990).
25) Rana T. M., Meares C. F., *Proc. Nat. Acad. Sci. U.S.A.*, **88**, 10578—10582 (1991).
26) Puchara M., Schuessler H., *Int. J. Peptide Protein Res.*, **46**, 326—332 (1995).
27) Davis K. J. A., Lin S. W., Pacific R. E., *J. Biol. Chem.*, **262**, 9914—9920 (1987).
28) Walff S. P., Dean R. T., *Biochem. J.*, **234**, 399—403 (1986).
29) Halliwell B., Gutteridge J. M. C., *Arch. Biochem. and Biophys.*, **246**, 501—514 (1986).
30) Halliwell B., Gutteridge J. M. C., Aruoma O. I., *Anal. Biochem.*, **165**, 215—219 (1987).
31) Parij N., Nagy A. N., Neve J., *Free Rad. Res.*, **23**, 571—579 (1995).
32) Hu M. L., Chen Y. K., Lin Y. F., *Chem-Biol. Interact.*, **97**, 63—73 (1995).
33) Sugita M., Yatsuhashi M., Shimada T., Inoue H., *Res. Chem. Intermed.*, to be submitted.
34) Das D., Bandyopadhyay D., Bhattacharjee M., Banerjee R., *Free Rad. Biol. & Med.*, **23**, 8—18 (1997).
35) Tsai L., Lee K., Liu T., *Free Rad. Biol. & Med.*, **24**, 732—737 (1998).
36) Jahnke L. S., *Anal. Biochem.*, **269**, 273—277 (1999).
37) Fukai S., "New Drugs Today," 6th ed., Yakujijihou-sha, Japan, **1995**, pp.1—77.
38) Seelig A., Gottschilich R., Devant R. M., *Proc. Natl. Acad. Sci. U.S.A.*, **91**, 68—72 (1994).
39) Hammond J. R., Jarvis S. M., Paterson A. R. P., Clanachan A. S., *Biochem. Pharmacology*, **32**, 1229—1235 (1983).
40) Kragie L., Doyle D., *Endocrinology*, **130**, 1211—1216 (1992).
41) Dubey R. K., McAllister C. B., Inoue M., Wilkinson G. R., *J. Clin. Invest.*, **84**, 1155—1159 (1989).